Organic & Biomolecular Chemistry

www.rsc.org/obc

Volume 8 | Number 3 | 7 February 2010 | Pages 481–716

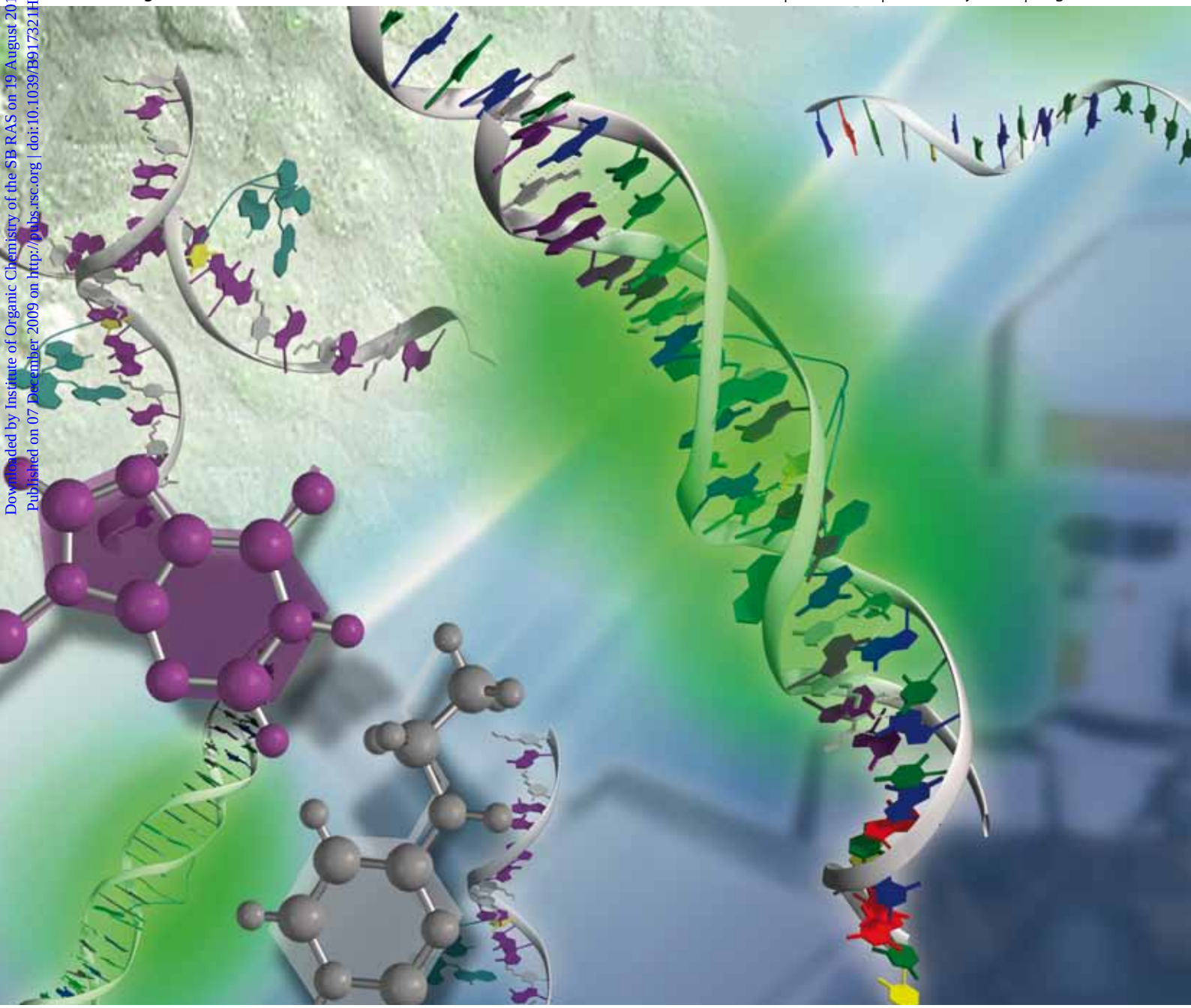

ISSN 1477-0520

RSC Publishing

1477-0520(2010)8:3;1-H

Hybridization-sensitive fluorescent DNA probe with self-avoidance ability†

Shuji Ikeda, Takeshi Kubota, Mizue Yuki, Hiroyuki Yanagisawa, Shizuho Tsuruma and Akimitsu Okamoto*

Received 21st August 2009, Accepted 31st October 2009
First published as an Advance Article on the web 7th December 2009
DOI: 10.1039/b917321h

Hybridization-sensitive fluorescent probes have an inherent disadvantage: self-dimerization of the probe prevents the fluorescence quenching prior to hybridization with the target, resulting in a high background signal. To avoid self-dimerization of probes, we focused on a base pair formed by 2′-deoxyinosine (I) and N^4-ethyl-2′-deoxycytidine (E). I and E bases form more stable base pairs with cytosine and guanine, respectively, compared with an I/E base pair. New hybridization-sensitive fluorescent probes, IE probes, were prepared containing three unnatural nucleotides, I, E and D_{514} as a doubly thiazole orange-labeled nucleotide. The IE probes had low thermostability, sufficient to avoid self-dimerization. Absorption spectra of the IE probes exhibited a hybridization-dependent shift of the absorption maximum, suggesting that excitonic interaction was working between the thiazole orange dyes in the probe. Interdye excitonic interaction of IE probes was very effective; thus, replacement of guanine and cytosine with I and E improved the ratio of fluorescence intensities after and before hybridization ($I_{hybrid}/I_{nonhybrid}$). Although a significant weakness in fluorescence intensity was observed for several IE probes after hybridization with the target sequence when both or either of the bases adjacent to D_{514} is E, a dramatic recovery of the fluorescence intensity of hybrids was observed when any E adjacent to D_{514} was replaced with cytosine. Improvement of the $I_{hybrid}/I_{nonhybrid}$ value by incorporation of I and E helped the design of a long probe sequence for mRNA imaging.

Introduction

Many fluorescent nucleic acid probes have been developed for observation of the functions of target nucleic acids.[1–3] In particular, a great deal of effort has been invested in the rational design of hybridization-sensitive fluorescent probes to detect effectively the target nucleic acid using on–off switching of fluorescence depending on hybridization.[4–12] A recently reported new type of hybridization-sensitive probe has a doubly fluorescence-labeled nucleotide to achieve high fluorescence intensity for a hybrid with the target nucleic acid and effective quenching for a single-stranded state of the probe.[13–16] Two thiazole orange dyes have been linked covalently to a single nucleotide in a DNA probe (D_{514}, Fig. 1). An excitonic interaction was produced by the formation of an H-aggregate between dyes, and as a result, emission from the probe before hybridization was suppressed. Dissociation of dye aggregates by hybridization with the complementary nucleic acid resulted in the disruption of excitonic interaction and a strong emission from the hybrid. However, hybridization-sensitive fluorescent probes have an inherent disadvantage, namely, fluorescence emission from the self-dimer of the probes.[14] Full or partial self-dimerization of the probe prevents the fluorescence-quenching function of the probe that does not recognize the target. The "self-dimer" formed by the probe may be thermodynamically unstable or imaginary because it contains many mismatched base pairs. However, this possible structure limits the design of highly hybridization-sensitive probes and demands prior estimation of the fluorescence properties of the probes. Incorporation of a self-avoidance ability into the structure of hybridization-sensitive fluorescence probes is required to remove the root cause of self-dimerization and improve the function of fluorometric nucleic acid detection.

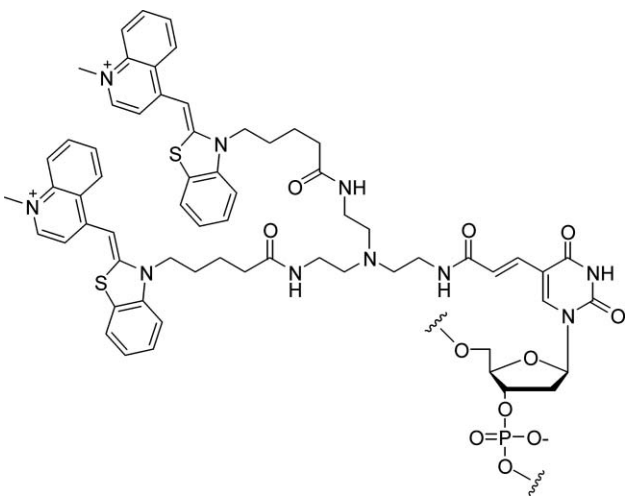

Fig. 1 Fluorescent nucleotide D_{514} controlled by excitonic interaction between thiazole orange dyes for an effective hybridization probe.

Here, we report the photophysical properties and application of newly designed DNA probes avoiding self-dimerization. The new probes showed unambiguous fluorescence switching depending on nucleic acid hybridization. The long probe prepared based on this concept made it possible to take an image of the target mRNA in a living cell.

RIKEN Advanced Science Institute, Wako, Saitama, 351-0198, Japan. E-mail: aki-okamoto@riken.jp; Fax: +81 48 467 9238; Tel: +81 48 467 9205

† Electronic supplementary information (ESI) available: Photophysical data of doubly thiazole orange-labeled probes hybridized with the complementary DNA and RNA. See DOI: 10.1039/b917321h

Table 1 Photophysical properties of doubly thiazole orange-labeled probes hybridized with the complementary DNA strands[a].

Probe sequences	Complementary	Absorption/nm (ε)		λ_{em}/nm (λ_{ex}/nm)	Quantum yields	$I_{hybrid}/I_{nonhybrid}$ (λ/nm)	T_m/°C[b]
CGCAAGD$_{514}$GAACGC	No addition	511 (53 000)	482 (38 000)	535 (516)	0.20		
	GCGTTCACTTGCG	511 (67 000)		529 (515)	0.40	2.2 (529)	70
EIEAAID$_{514}$IAAEIE	No addition	509 (43 000)	478 (88 000)	534 (516)	0.022		
	GCGTTCACTTGCG	510 (84 000)	481 (61 000)	529 (514)	0.36	22 (529)	42
CGCAATD$_{514}$TAACGC	No addition	510 (47 000)	480 (61 000)	534 (519)	0.059		
	GCGTTAAATTGCG	509 (79 000)		528 (513)	0.28	9.5 (528)	62
EIEAATD$_{514}$TAAEIE	No addition	509 (61 000)	479 (99 000)	539 (521)	0.015		
	GCGTTAAATTGCG	509 (100 000)	482 (79 000)	528 (512)	0.19	40 (528)	43
AGATCCD$_{514}$GACAGA	No addition	510 (110 000)	483 (70 000)	531 (514)	0.27		
	TCTGTCAGGATCT	509 (120 000)		529 (514)	0.41	1.6 (529)	67
AIATEED$_{514}$IAEAIA	No addition	507 (51 000)	480 (56 000)	533 (515)	0.022		
	TCTGTCAGGATCT	508 (60 000)	482 (50,000)	533 (513)	0.15	8.4 (533)	40
AIATECD$_{514}$IAEAIA	No addition	506 (74 000)	479 (96 000)	536 (512)	0.027		
	TCTGTCAGGATCT	510 (120 000)		528 (514)	0.35	21 (528)	49
TCTTGCD$_{514}$CGAAGT	No addition	509 (90 000)	483 (80 000)	536 (516)	0.13		
	ACTTCGAGCAAGA	509 (120 000)		530 (514)	0.40	3.7 (530)	69
TETTIED$_{514}$EIAAIT	No addition	509 (69 000)	477 (120 000)	537 (515)	0.021		
	ACTTCGAGCAAGA	509 (83 000)	478 (110 000)	532 (514)	0.17	12 (532)	37
TETTICD$_{514}$CIAAIT	No addition	506 (65 000)	478 (120 000)	536 (516)	0.025		
	ACTTCGAGCAAGA	510 (120 000)		531 (514)	0.39	34 (531)	52
<mismatched>							
EIEAAID$_{514}$IAAEIE	GCGTTCTCTTGCG	507 (62 000)	479 (77 000)	532 (514)	0.15	7.3 (532)	34
	GCGTTCGCTTGCG	508 (45 000)	477 (93 000)	534 (514)	0.035	1.1 (534)	17
	GCGTTCCCTTGCG	507 (47 000)	478 (89 000)	532 (514)	0.047	1.4 (534)	25
	GCCTTGAGTTCCG	507 (43 000)	477 (89 000)	534 (517)	0.017	0.97 (534)	<10

[a] 0.4 μM hybrid, 50 mM sodium phosphate buffer (pH = 7.0), 100 mM sodium chloride, except T_m measurements. [b] 2.0 μM hybrid, 50 mM sodium phosphate buffer (pH = 7.0), 100 mM sodium chloride.

Results and discussion

Probe design and preparation

To avoid self-dimerization of probes, control of the thermostability of the probe dimer should be considered. The key point is to weaken the interaction between probes, in particular, to weaken the relatively strong guanine–cytosine hydrogen bonds, while maintaining sufficient hydrogen-bonding ability to hybridize with the target nucleic acid. In view of this concept on the control of thermostability, we focused on a base pair formed by 2′-deoxyinosine (I) and N^4-ethyl-2′-deoxycytidine (E) (Fig. 2). I and E bases form more stable base pairs with cytosine and guanine, respectively, than with an I/E base pair.[17–19] The base combination is expected to enable multiplexed PCR by avoiding any undesired primer–primer interactions. We incorporated this base pairing system to the new probe to avoid probe dimerization. Simultaneously, this modified probe requires the function of the on–off switching of fluorescence emission in sensitive response to nucleic acid recognition, based on interdye excitonic interaction. Therefore, we prepared a new hybridization-sensitive probe that contains three unnatural nucleotides: I as a surrogate of 2′-deoxyguanosine, E as a surrogate of 2′-deoxycytidine and D$_{514}$ as a functional fluorescent nucleotide. Phosphoramidites of I, E and the precursor of D$_{514}$ were used for a conventional DNA synthesis method.[13] The list of synthesized fluorescent DNA probes and their physical properties is shown in Table 1 and Table S1 in the ESI.†

Thermostability

The T_m values of the hybrids of our new fluorescent probes (IE probes) with the complementary DNA strands (2 μM) were initially measured in a phosphate buffer (pH = 7.0) and compared with those of "natural" fluorescent probes (GC probe). The absorbance of the hybrids was monitored at 260 nm from 10 to 90 °C, and the first derivatives were calculated to determine the value of T_m from these profiles. The hybrid of the IE probe with the complementary strand was thermally stable (Table 1), but showed 3–5 °C lower T_m value per modified nucleotide compared with the T_m of the corresponding GC probe-used hybrid. The sigmoidal curve of absorbance change was not observed, which arises from dimerization of IE probes; thus, the T_m of the probe dimer is expected to be low enough to avoid self-dimerization.

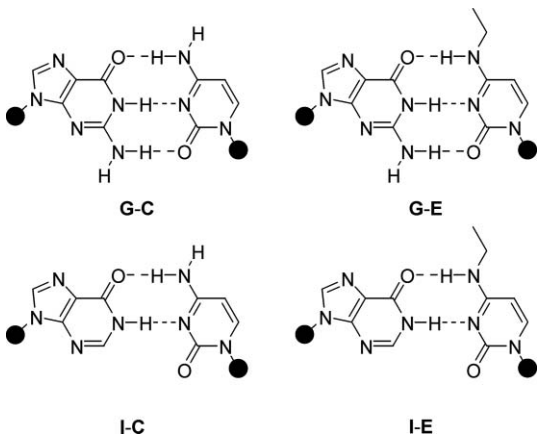

Fig. 2 Four possible base pairs with 2′-deoxyguanosine (G), 2′-deoxyinosine (I), 2′-deoxycytidine (C) and N^4-ethyl-2′-deoxycytidine (E).

Photophysical properties

A new type of probe structure is required that avoids self-dimerization and maintains the hybridization-sensitive on–off fluorescence switching function. We next measured the absorption and emission spectra of IE probes before and after hybridization with the complementary strands. Absorption spectra of the IE probes exhibited a hybridization-dependent shift of absorption maxima. For example, the absorption bands of EIEAAID$_{514}$IAAEIE appeared at 482 and 511 nm when probes were in a solution without the complementary DNA strand, whereas an absorption band at a longer wavelength (511 nm) became predominant when the probe was hybridized with the complementary strand, GCGTTCACTTGGG (Fig. 3). The shift of absorption maxima can be explained in terms of the exciton coupling theory,[20] in which the excited state of the dye H-aggregate[21–23] splits into two energy levels (Fig. 4). The transition to the upper excitonic state is allowed for the H-aggregates, which rapidly deactivate to the lower excitonic state. However, emission from the lower energy level is forbidden. On the other hand, hybridization with the complementary strand results in dissociation of dye aggregates. The aggregate dissociation at the hybridized state was indicated by a shift of the absorption maximum to a longer wavelength. Disruption of the excitonic interaction in the aggregate gave strong emission from the hybrid. Therefore, the emission intensity of the IE probes before hybridization was weak, but the emission spectra of the probes hybridized with the target DNA strands were observed at approximately 530 nm as a single broad band. This hybridization-dependent fluorescence switching of IE probes is almost the same as that of GC probes reported earlier.[13]

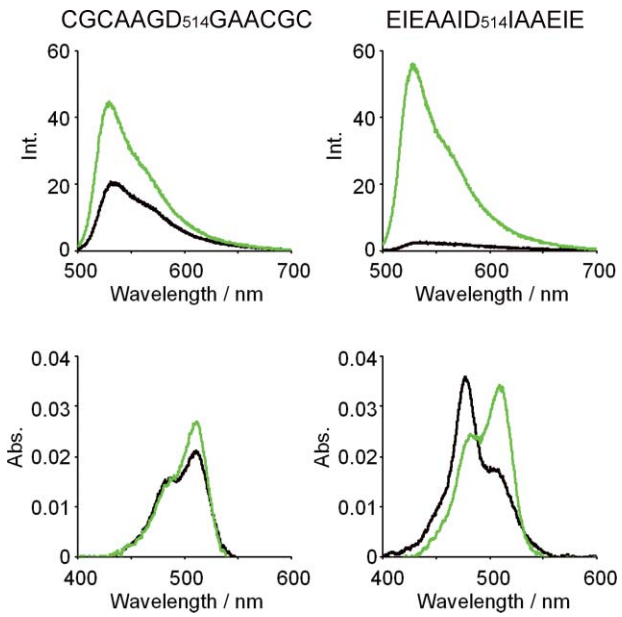

Fig. 3 Emission and absorption spectra. Left panels show the spectra of CGCAAGD$_{514}$GAACGC and right panels show the spectra of EIEAAID$_{514}$IAAEIE. Emission spectra are shown in the top panels and absorption spectra are shown in the bottom panels. Spectra were measured in 50 mM sodium phosphate buffer (pH = 7.0) containing 100 mM sodium chloride at 25 °C. Black, spectra before hybridization; green, spectra after hybridization with the corresponding complementary DNA. Emission spectra were recorded with excitation at 488 nm.

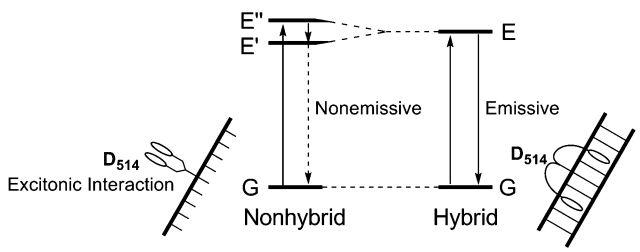

Fig. 4 Schematic representation of the energy levels of the single- and double-stranded states of the hybridization probe controlled by excitonic interaction between thiazole orange dyes.

In spite of the probe design based on interdye excitonic interaction, a low ratio of fluorescence intensities after and before hybridization ($I_{hybrid}/I_{nonhybrid}$) has so far often been observed for GC probes because of the high fluorescence intensity before hybridization. However, replacement of guanine and cytosine with I and E improved $I_{hybrid}/I_{nonhybrid}$. For example, a GC probe CGCAAGD$_{514}$GAACGC showed $I_{hybrid}/I_{nonhybrid}$ = 2.2. When all guanines and cytosines were replaced with I and E, $I_{hybrid}/I_{nonhybrid}$ values increased to 22. Replacement of GC probes CGCAATD$_{514}$TAACGC ($I_{hybrid}/I_{nonhybrid}$ = 9.5) and AGATCCD$_{514}$GACAGA ($I_{hybrid}/I_{nonhybrid}$ = 1.6) with I and E also produced a dramatic increase in $I_{hybrid}/I_{nonhybrid}$ values ($I_{hybrid}/I_{nonhybrid}$ = 40 and 8.4, respectively). Enhancement of $I_{hybrid}/I_{nonhybrid}$ is due to suppression of the fluorescence emission of IE probes in the absence of the complementary strands. Incorporation of the IE system to hybridization-sensitive probes effectively avoids fluorescence emission by self-dimerization. Absorption at shorter wavelength (480 nm), which indicates aggregation of thiazole orange dyes, was enhanced in the absorption spectra of IE probes in the absence of complementary DNA, compared with absorption at longer wavelength (510 nm). For example, CGCAAGD$_{514}$GAACGC and AGATCCD$_{514}$GACAGA showed A_{480}/A_{510} = 0.69 and 0.57, respectively. When their guanines and cytosines were replaced with I and E, the A_{480}/A_{510} values changed to 2.15 and 1.16, respectively. Enhancement of the A_{480}/A_{510} value indicates that excitonic interaction by intramolecular dye aggregation works in the probe in the absence of the complementary DNA. Incorporation of I and E into probes may make it difficult to form the self-dimer that promotes dissociation of the dye aggregate structure.

Mismatched base pairs strongly suppress fluorescence emission. For example, the hybrid of the IE probe, EIEAAID$_{514}$IAAEIE, with the complementary DNA containing a mismatched base pair at D$_{514}$, GCGTTC*N*CTTGCG (*N* = T, C, or G), was thermally unstable, and showed a much lower T_m value compared with that of the full-matched hybrid. The decrease in T_m values by mismatched base pair formation results in low fluorescence emission. When the T_m value was lower than the temperature used in the fluorescence measurement (25 °C), we observed little increase in fluorescence intensity. The mismatched base pair formation at E and I also contributes to the suppression of fluorescence intensity, because the T_m value decreases significantly. The rise of the fluorescent intensity is not observed even if a mismatched strand, such as GCCTTGAGTTCCG, is added into a solution of EIEAAID$_{514}$IAAEIE.

Effect of adjacent ethylcytosine

Although the fluorescence of the IE probe was effectively suppressed in the absence of the complementary DNA, a significant weakness in fluorescence intensity was often observed for several IE probes in spite of addition of the complementary DNA. The common feature of such IE probes is that both or either of the bases adjacent to D_{514} is E. For example, the fluorescence intensity of AIATEED$_{514}$IAEAIA/TCTGTCAGGATCT was only 26% of that of the corresponding GC probe (Fig. 5). The fluorescence intensity of TETTIED$_{514}$EIAAIT/ACTTCGAGCAAGA was also only 22% of that of the corresponding GC probe. These absorption spectra showed the feature that the absorption band at the shorter wavelength remains relatively strong even after hybridization with the complementary DNA. The strong absorption at shorter wavelength after hybridization suggests that the dissociation of the dye aggregate is inefficient. GC probes emit fluorescence after hybridization by dissociation of the aggregate and subsequent binding of dye to DNA structure from the major groove side, whereas the absorption spectra of IE probes indicate that the probe cannot do that. The N^4-ethyl group of E juts out into the major groove of the duplex structure of the hybrid. This ethyl group would sterically disturb the binding of dye to the DNA structure. As a result, dyes would keep an aggregation form even after hybridization, which suppresses fluorescence emission.

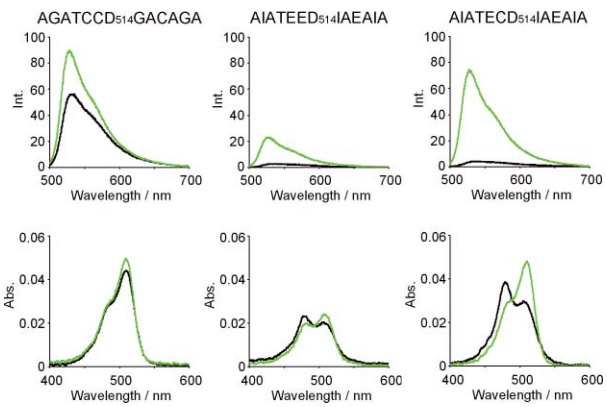

Fig. 5 Adjacent ethylcytosine effect. Left panels show the spectra of AGATCCD$_{514}$GACAGA, center panels show the spectra of AIATEED$_{514}$IAEAIA and right panels show the spectra of AIATECD$_{514}$IAEAIA. Emission spectra are shown in the top panels and absorption spectra are shown in the bottom panels. Spectra were measured in 50 mM sodium phosphate buffer (pH = 7.0) containing 100 mM sodium chloride at 25 °C. Black, spectra before hybridization; green, spectra after hybridization with the corresponding complementary DNA. Emission spectra were recorded with excitation at 488 nm.

To avoid a decrease in the fluorescence intensity of hybrids, any E adjacent to D_{514} was replaced with cytosine. Changing E adjacent to D_{514} to cytosine resulted in a dramatic recovery of fluorescence intensity after hybridization. For example, the fluorescence intensity of the hybrid with an IE probe, AIATECD$_{514}$IAEAIA/TCTGTCAGGATCT, was dramatically improved to 83% of that with the corresponding GC probe, and this probe showed very effective on–off fluorescence switching ability ($I_{hybrid}/I_{nonhybrid}$ = 21 for the new IE probe and 1.6 for the GC probe). The fluorescence intensity of another hybrid TETTICD$_{514}$CIAAIT/ACTTCGAGCAAGA also increased up to 79% of that with the corresponding GC probe, and a high $I_{hybrid}/I_{nonhybrid}$ value was obtained ($I_{hybrid}/I_{nonhybrid}$ = 34 for the new IE probe and 3.7 for the GC probe).

Hybridization with RNA and application to live cell RNA imaging

IE probes are also effective for fluorometric detection of RNA. Although the thermostabilities of IE probe–RNA hybrids were lower than those of probe–DNA hybrids, strong fluorescence intensities and high $I_{hybrid}/I_{nonhybrid}$ values were obtained (ESI, Table S2†). The $I_{hybrid}/I_{nonhybrid}$ values of IE probes were much higher than those of the corresponding GC probes.

Improvement of $I_{hybrid}/I_{nonhybrid}$ values by incorporation of I and E helps the design of a long probe sequence for mRNA imaging. Fluorescent probes with a long sequence have high binding ability to the target nucleic acid and also can recognize a long target sequence at once. However, long single-stranded probes often contain secondary and tertiary structures, and partly form self-dimers. These higher-ordered structures of probes impair the performance of the probe function. Accessibility to the target sequences drops off and fluorescence is emitted regardless of hybridization with the target strand. However, the IE probe would give us an effective solution.

Actually, the 50-nt IE probe showed clear on–off fluorescence switching depending on hybridization with the complementary RNA, which is different from the fluorescence behavior of the 50-nt GC probe. We prepared a 50-nt IE probe for detection of β-actin mRNA (**Probe514**) (Fig. 6). Sharper on–off fluorescent switching of the IE probe was initially confirmed before and after addition of the target RNA to the probe solution ($I_{hybrid}/I_{nonhybrid}$ = 5.5), compared with the corresponding GC probe ($I_{hybrid}/I_{nonhybrid}$ = 3.8).

We next applied **Probe514** together with another hybridization-sensitive probe TTTTTTD$_{600}$TTTTTT (**Probe600**), which emits fluorescence at 630 nm when the probe binds to mRNA polyA tail,[24] to living HeLa cells using manipulator-assisted microinjection to visualize intracellular β-actin mRNA. Immediately after injection of the probes to the cytoplasm area, fluorescence from **Probe514** was observed, mainly from the cytoplasm area. The fluorescence was stronger in the area closer to the cell edge. The distribution pattern of fluorescence of **Probe514** was similar to the results reported previously on β-actin mRNA distribution.[25–29] Fluorescence from **Probe600** was observed from all over the cell, being particularly strong from the nucleus area. The marked change in the photophysical behavior of IE probes that are dependent on RNA strands played a key role in fluorescence imaging of the target RNA expressed in a living cell.

Conclusion

We have described self-avoiding probes for the function of on–off switching of fluorescence emission in sensitive response to nucleic acid recognition. The IE probes that we synthesized showed higher fluorescence suppression based on interdye excitonic interaction before hybridization with the complementary nucleic acid. This contrasts with the low fluorescence suppression of GC probes in the absence of the complementary nucleic acid. Furthermore, IE probes retained a higher fluorescent intensity after hybridization. The IE probe enables us to design a hybridization-sensitive

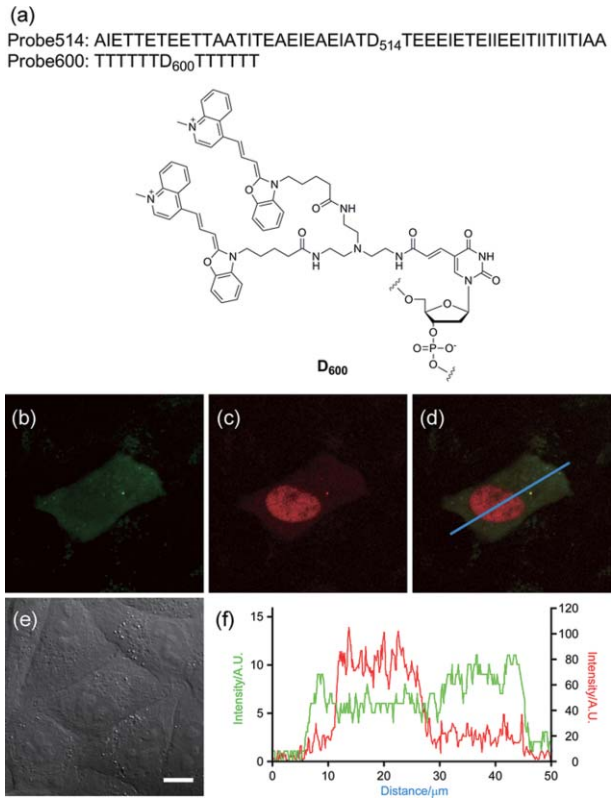

Fig. 6 Long IE probe and its application to imaging of β-actin mRNA. (a) Probe sequences. (b) A fluorescence image of a probe-microinjected HeLa cell (**Probe514** for β-actin mRNA). The sample was excited at 488 nm and the fluorescence was collected through a 505 nm long-pass filter. (c) A fluorescence image of a probe-microinjected HeLa cell (**Probe600** for mRNA polyA tail). The sample was excited at 543 nm and the fluorescence was collected through a 615 nm long-pass filter. (d) Merge of panels (b) and (c). (e) Differential interference contrast. Bar, 10 μm. (f) Intensity profiles along the blue line in panel (d); green line, fluorescence from **Probe514**; red line, fluorescence from **Probe600**.

probe with a long sequence and facilitates taking the image of endogenous mRNA in living cells. The present probe resolved the issue of low on–off fluorescence switching by nucleobase modification and now we anticipate that it will be a practical tool for effective monitoring of the spatiotemporal characteristics of RNAs in living cells.

Experimental

General

DNA was synthesized on an Applied Biosystems 392 DNA/RNA synthesizer or an NTS H-6 DNA/RNA synthesizer. Reversed-phase HPLC was performed on CHEMCOBOND 5-ODS-H columns (10 × 150 mm) with a Gilson Chromatograph, Model 305, using a UV detector, Model 118, at 260 nm. MALDI-TOF mass spectra were measured with a Bruker Daltonics Reflex. UV and fluorescence spectra were recorded on a Shimadzu UV-2550 spectrophotometer and RF-5300PC spectrofluorophotometer, respectively.

Probe synthesis

DNA oligomers were synthesized by a conventional phosphoramidite method on a DNA/RNA synthesizer. Commercially available phosphoramidites were used for dA, dG, dC, dT, 2′-deoxyinosine, and N^4-ethyl-2′-deoxycytidine. The synthesized phosphoramidite of N^4-ethyl-2′-deoxycytidine was also used.[30] The diamino-modified nucleoside phosphoramidite, which was modified with thiazole orange dyes, was synthesized according to our previous report.[13] The synthesized DNA oligomer was cleaved from the support with 28% aqueous ammonia or 2 M ammonia in methanol and deprotected at 25 °C for 16 h. After removal of ammonia from the solution under reduced pressure, the DNA was purified by reversed-phase HPLC, elution with a solvent mixture of 0.1 M triethylammonium acetate (TEAA) (pH = 7.0), and linear gradient over 20 min from 5% to 30% acetonitrile at a flow rate of 3.0 mL min^{-1}. For determination of the concentration of each DNA, the purified DNA was fully digested with calf intestine alkaline phosphatase (50 U mL^{-1}) and P1 nuclease (50 U mL^{-1}) at 25 °C for 16 h. Digested solutions were analyzed by HPLC, elution with a solvent mixture of 0.1 M TEAA (pH = 7.0), and linear gradient over 20 min from 3% to 10% acetonitrile at a flow rate of 3.0 mL min^{-1}. The concentration was determined by comparing peak areas with a standard solution containing dA, dC, dG, and dT at concentrations of 0.1 mM. A solution of the succinimidyl ester of thiazole orange pentanoic acid[13] (50 equiv. to an active amino group of DNA) in DMF was added to a solution of deprotected DNA in 100 mM sodium carbonate buffer (pH = 9.0), and incubated at 25 °C for 10 min. The reaction mixture was diluted with ethanol. After centrifuging at 4 °C for 20 min, the supernatant liquid was removed. The residue was dissolved in a small amount of water and then the solution was passed through a 0.45 μm filter. The product was purified by reversed-phase HPLC on a 5-ODS-H column, elution with a solvent mixture of 0.1 M TEAA (pH = 7.0), and linear gradient over 28 min from 5% to 40% acetonitrile at a flow rate of 3.0 mL min^{-1}). The concentration of the fluorescent DNA was determined by the same method as described in the DNA synthesis. The fluorescent DNA was identified by MALDI-TOF mass spectrometry (here, the molecular weight of the counter anions of dyes is not included in the value of M, and D_{514} denotes a doubly thiazole orange-labeled deoxynucleotide.): CGCAATD$_{514}$TAACGC, calcd for $C_{180}H_{217}N_{56}O_{78}P_{12}S_2$ ([M–H]$^+$) 4848.8, found 4851.4; EIEAATD$_{514}$TAAEIE, calcd for $C_{188}H_{231}N_{54}O_{78}P_{12}S_2$ ([M–H]$^+$) 4931.0, found 4932.3; CGCAAGD$_{514}$GAACGC, calcd for $C_{180}H_{215}N_{62}O_{76}P_{12}S_2$ ([M–H]$^+$) 4898.8, found 4897.8; EIEAAID$_{514}$IAAEIE, calcd for $C_{188}H_{227}N_{58}O_{76}P_{12}S_2$ ([M–H]$^+$) 4951.0, found 4952.6; AGATCCD$_{514}$GACAGA, calcd for $C_{181}H_{216}N_{61}O_{76}P_{12}S_2$ ([M–H]$^+$) 4897.9, found 4899.5; AIATEED$_{514}$IAEAIA, calcd for $C_{187}H_{225}N_{58}O_{76}P_{12}S_2$ ([M–H]$^+$) 4937.0, found 4939.4; AIATECD$_{514}$IAEAIA, calcd for $C_{185}H_{221}N_{58}O_{76}P_{12}S_2$ ([M–H]$^+$) 4912.0, found 4911.4; GAGTTCD$_{514}$CTACTA, calcd for $C_{181}H_{219}N_{52}O_{81}P_{12}S_2$ ([M–H]$^+$) 4854.8, found 4856.7; IAITTED$_{514}$ETAETA, calcd for $C_{187}H_{229}N_{50}O_{81}P_{12}S_2$ ([M–H]$^+$) 4909.0, found 4910.7; IAITTCD$_{514}$CTAETA, calcd for $C_{183}H_{221}N_{50}O_{81}P_{12}S_2$ ([M–H]$^+$) 4852.9, found 4852.7; ATTATGD$_{514}$CAGACT, calcd for $C_{182}H_{219}N_{54}O_{80}P_{12}S_2$ ([M–H]$^+$) 4878.9, found 4880.3;

ATTATID$_{514}$EAIAET, calcd for $C_{186}H_{225}N_{52}O_{80}P_{12}S_2$ ([M–H]$^+$) 4904.9, found 4905.7; ATTATID$_{514}$CAIAET, calcd for $C_{184}H_{221}N_{52}O_{80}P_{12}S_2$ ([M–H]$^+$) 4876.9, found 4878.4; AGCTTCD$_{514}$CCTTAA, calcd for $C_{180}H_{219}N_{50}O_{81}P_{12}S_2$ ([M–H]$^+$) 4814.8, found 4816.5; AIETTED$_{514}$EETTAA, calcd for $C_{188}H_{234}N_{49}O_{81}P_{12}S_2$ ([M–H]$^+$) 4912.0, found 4913.6; AIETTCD$_{514}$CETTAA, calcd for $C_{184}H_{226}N_{49}O_{81}P_{12}S_2$ ([M–H]$^+$) 4855.9, found 4858.3; TCTTGCD$_{514}$CGAAGT, calcd for $C_{181}H_{219}N_{52}O_{82}P_{12}S_2$ ([M–H]$^+$) 4870.8, found 4872.9; TETTIED$_{514}$EIAAIT, calcd for $C_{187}H_{228}N_{49}O_{82}P_{12}S_2$ ([M–H]$^+$) 4910.0, found 4911.8; TETTICD$_{514}$CIAAIT, calcd for $C_{183}H_{220}N_{49}O_{82}P_{12}S_2$ ([M–H]$^+$) 4853.8, found 4855.7; AGCTTCTCCTTAATGTCACGCACGATD$_{514}$TCCCGCTCGGCCGTGGTGGTGAA, calcd for $C_{539}H_{672}N_{186}O_{307}P_{49}S_2$ ([M–H]$^+$) 16250.0, found 16249.9; AIETTETEETTAATITEAEIEAEIATD$_{514}$TEEEIETEIIEEITIITIITIAA, calcd for $C_{569}H_{719}N_{173}O_{307}P_{49}S_2$ ([M–H]$^+$) 16475.6, found 16478.7.

Absorption and fluorescence measurements

Absorption and fluorescence spectra of the fluorescent probes (0.4 μM) were measured in 50 mM sodium phosphate buffer (pH 7.0) containing 100 mM sodium chloride using a cell with a 1 cm path length. The excitation and emission bandwidths were 1.5 nm.

Melting temperature measurements

The T_m values of duplexes (2.0 μM) were measured in 50 mM sodium phosphate buffer (pH = 7.0) containing 100 mM sodium chloride. The absorbance of the samples was monitored at 260 nm from 10 to 90 °C with a heating rate of 0.5 °C min^{-1}. From these profiles, first derivatives were calculated to determine the value of T_m.

Cell culture

Dulbecco's modified Eagle's medium (DMEM) and fetal bovine serum (FBS) were purchased from GIBCO. Reagents for culturing were from Sigma. HeLa cells were cultured at 37 °C in DMEM containing 10% heat-inactivated FBS, 25 U mL^{-1} penicillin and 25 mg mL^{-1} streptomycin, under a humidified atmosphere with 5% CO_2. For experimental use, cells (passage number 5–9) were cultured in glass-base dishes (Matsunami). Before microscope observation, the culture medium was washed and exchanged to phenol red-free DMEM. Cells were maintained in a culturing condition by an incubation system (INU; Tokai Hit) during observation.

Live cell imaging

Images were acquired with a motorized inverted microscope (Axio Observer Z1; Zeiss) equipped with an objective (PlanApochromat 63× oil immersion NA 1.4). Differential interference contrast and fluorescent images were acquired with a confocal unit LSM 510 META (Zeiss) equipped with Ar and He–Ne lasers. Acquired images were analyzed and processed with Zeiss software (ZEN 2007, Zeiss). A mixture of **Probe514** (10 μM) and **Probe600** (10 μM) dissolved in water was microinjected using a pneumatic injector (FemtoJet express; Eppendorf) with glass needles (FemtoTip; Eppendorf) and 3-D manipulators (Narishige). Injection was performed at 130 hPa for 0.5 s in the cell (*ca.* 100–500 fL). **Probe514** was excited with 488 nm irradiation and detected through a 505LP filter, and **Probe600** was excited with 543 nm irradiation and detected through a 615LP filter.

Acknowledgements

We thank Dr Takehiro Suzuki (Biomolecular Characterization Team, RIKEN) for the MALDI-TOF mass spectrometry.

Notes and references

1 S. Paillasson, M. van de Corput, R. W. Dirks, H. J. Tanke, M. Robert-Nicoud and X. Ronot, *Exp. Cell Res.*, 1997, **231**, 226.
2 U. Asseline, *Curr. Org. Chem.*, 2006, **10**, 491.
3 A. A. Martí, S. Jockusch, N. Stevens, J. Ju and N. J. Turro, *Acc. Chem. Res.*, 2007, **40**, 402.
4 S. Tyagi and F. R. Kramer, *Nat. Biotechnol.*, 1996, **14**, 303.
5 R. Lartia and U. Asseline, *Chem.–Eur. J.*, 2006, **12**, 2270.
6 D. V. Jarikote, O. Köhler, E. Socher and O. Seitz, *Eur. J. Org. Chem.*, 2005, 3187.
7 V. L. Marin and B. A. Armitage, *Biochemistry*, 2006, **45**, 1745.
8 C. E. Kerr, C. D. Mitchell, Y. M. Ying, B. E. Eaton and T. L. Netzel, *J. Phys. Chem. B*, 2000, **104**, 2166.
9 A. Okamoto, K. Tainaka and I. Saito, *J. Am. Chem. Soc.*, 2003, **125**, 4972.
10 A. Okamoto, K. Tanaka, T. Fukuta and I. Saito, *J. Am. Chem. Soc.*, 2003, **125**, 9296.
11 A. Okamoto, K. Kanatani and I. Saito, *J. Am. Chem. Soc.*, 2004, **126**, 4820.
12 A. Okamoto, Y. Saito and I. Saito, *J. Photochem. Photobiol., C*, 2005, **6**, 108.
13 S. Ikeda and A. Okamoto, *Chem.–Asian J.*, 2008, **3**, 958.
14 S. Ikeda, T. Kubota, K. Kino and A. Okamoto, *Bioconjugate Chem.*, 2008, **19**, 1719.
15 T. Kubota, S. Ikeda and A. Okamoto, *Bull. Chem. Soc. Jpn.*, 2009, **82**, 110.
16 T. Kubota, S. Ikeda, H. Yanagisawa, M. Yuki and A. Okamoto, *Bioconjugate Chem.*, 2009, **20**, 1256.
17 J. Woo, R. B. Meyer and H. B. Gamper, *Nucleic Acids Res.*, 1996, **24**, 2470.
18 G. Lahoud, V. Timoshchuk, A. Lebedev, M. de Vega, M. Salas, K. Arar, Y.-M. Hou and H. Gamper, *Nucleic Acids Res.*, 2008, **36**, 3409.
19 S. Hoshika, F. Chen, N. A. Leal and S. A. Benner, *Nucleic Acids Symp. Ser.*, 2008, **52**, 129.
20 M. Kasha, *Radiat. Res.*, 1963, **20**, 55.
21 R. F. Khairutdinov and N. Serpone, *J. Phys. Chem. B*, 1997, **101**, 2602.
22 T. Sagawa, H. Tobata and H. Ihara, *Chem. Commun.*, 2004, 2090.
23 A. Fürstenberg, M. D. Julliard, T. G. Deligeorgiev, N. I. Gadjev, A. A. Vasilev and E. Vauthey, *J. Am. Chem. Soc.*, 2006, **128**, 7661.
24 S. Ikeda, T. Kubota, M. Yuki and A. Okamoto, *Angew. Chem., Int. Ed.*, 2009, **48**, 6480.
25 P. J. Santangelo, A. W. Lifland, P. Curt, Y. Sasaki, G. J. Bassell, M. E. Lindquist and J. E. Crowe Jr., *Nat. Methods*, 2009, **6**, 347.
26 S. Tyagi and O. Alsmadi, *Biophys. J.*, 2004, **87**, 4153.
27 M. A. Hill, L. Schedlich and P. Gunning, *J. Cell Biol.*, 1994, **126**, 1221.
28 E. H. Kislauskis, X. Zhu and R. H. Singer, *J. Cell Biol.*, 1997, **136**, 1263.
29 J. B. Lawrence and R. H. Singer, *Cell*, 1986, **45**, 407.
30 H.-K. Nguyen, P. Auffray, U. Asseline, D. Dupret and N. T. Thuong, *Nucleic Acids Res.*, 1997, **25**, 3059.